Seismic assessment of metallic neo-gothic church: deterioration and safety of early structural design

Georgios Vlachakis[1*], Nicole O'Hearne[1], Nuno Mendes[1], Paulo B. Lourenço[1]

[1]ISISE, Department of Civil Engineering, University of Minho, Guimarães, Portugal

[*]Correspondence to: Georgios Vlachakis, ISISE, Department of Civil Engineering, University of Minho, Campus de Azurém, Guimarães, 4800-058, Portugal; E-mail: giorgovlachaki@gmail.com

Seismic assessment of metallic neo-gothic church: deterioration and safety of early structural design

Abstract – The San Sebastian Basilica, located in Manila in Philippines, consists of a unique architectural monument in the area, representing the colonial neo-gothic style of the 19th century. The site where the church is constructed is characterized by high seismicity, and as an attempt to make it earthquake resistance, it was constructed by steel, after multiple collapses of previous versions of the church. The aim of this study is to assess the safety of the Basilica, by integrating an in-situ diagnostic campaign. More specifically, the investigation works performed in the last decade are enriched by experimental dynamic identification tests. After obtaining the dynamic properties of the church, a detailed numerical model is constructed and calibrated to match the experimental results. The final model is then employed and several non-linear static analyses are performed in order to assess the capacity of the church. A number of numerical and methodological issues are highlighted throughout the process, before concluding about the safety, the damage state and the main structural vulnerabilities of the Basilica.

Keywords: Steel monument; Dynamic identification test; Finite element modeling; Corrosion damage; Nonlinear static analysis; Seismic assessment

1. Introduction

Monumental constructions constitute a significant part of the built cultural heritage, and are often recognized to reflect our cultural identity and historical continuity. The societal effort given to protect and preserve their integrity has been embodied and formalized during the last centuries in several texts, charters and guidelines, see [1] for an overview of conservation evolution from an engineering perspective, namely with the ICOMOS/ISCARSAH recommendations [2]. Yet, the process needed for a decision making strategy might not be straightforward, as some key concepts, like authenticity, are subjective and vary depending on the cultural context [1]. Nevertheless, several objective criteria can be identified based on the conservation principles, while a case-depended integrated multi-disciplinary approach is required.

At the same time, the hazards to which the structure is exposed shall guide the choice of remedial measures [3]. Among other disasters, many seismic destructive events affected the built cultural heritage (e.g. earthquakes of Umbria-Marche 1997, Bam 2003, Kashmir 2005, Pisco 2007, L'Aquila 2009, Haiti 2010, Christchurch 2011, Lorca 2011, Emilia Romagna 2012, Nepal 2015, Central Italy 2016, Lesvos 2017, Mexico 2017). This seems to be often due to the lack of concern of original builders with extreme events and the lack of proper action from our societies with respect to risk management. Still, the seismic safety assessment of the built cultural heritage constitutes a particular challenging field of study, mainly due to the uncertainties involved [4], [5], [6], [7], [8]. Therefore, the ICOMOS recommendations not only suggest the integration of different diagnostic approaches, in order to conclude about the safety and the need of interventions, but also stress the relevance of the experts' opinion and personal judgment in the process. This paper presents an illustrative application to the Basilica of San Sebastian in Philippines, a unique architectural construction, built in an area of high seismicity, which is also a history of structural failures with churches affected due to disasters through the time of history. The current version is also at risk due to metal corrosion and this further justifies the current works.

The San Sebastian Basilica was constructed in Manila in Philippines at the end of the 19th century and has adopted the neo-gothic architecture of the era, although built with metal. It is characterized by particular historical significance, as it is the only fully prefabricated steel church in the Philippines (made in Belgium and steam-boated to Asia). It is also one of the few remaining churches in the Philippines that maintain its original design, interior finishes and materials. As a result, the Basilica was on the Tentative List to become a UNESCO World Heritage Site (although removed in 2015 due to structural decay), while it was declared a National Historical Landmark by the Philippine government in 1973 and a National Cultural Treasure in 2011. Moreover, it was included in the World Monuments Fund Watch list both in 1998 and 2010.

The archipelago of Philippines is located on the Pacific Ring of Fire and is characterized by high seismic activity [9]. As stated, the San Sebastian Basilica is the

fourth church built on the site, in the historic district of Quiapo, in Manila, since all three previous churches have been severely damaged or completely destroyed by earthquakes. In addition to the high seismic exposure, the church was showing important signs of deterioration. As a result, the Save San Sebastian Basilica Conservation and Development Inc. was founded in 2011 with the intention of preserving this unique construction through a ten-year restoration project. Since then, the Save Foundation has performed an extensive investigation plan in order to assess how the Basilica is deteriorating and the results have been presented in [10].

As a part of this effort, the University of Minho has conducted a safety assessment campaign of the Basilica, and the outcomes are presented in detail in this study. The scope of the campaign is to assess the safety of this complex construction and its current capacity with respect to the high seismic hazard. Firstly, the works include the execution of experimental dynamic identifications tests, aiming to estimate the main dynamic properties of the Basilica. The outcomes of the investigation works are then integrated into a detailed numerical model, and non-linear analyses are conducted. Several methodological and modeling issues are highlighted throughout the approach, before concluding about the structural safety of the church.

The outline of the paper is as follows: Section 2 presents the historical context of the Basilica, with a brief description of the structure; Section 3 summarizes the main outcomes of the previously performed investigations concerning the condition of the church, and in addition includes the experimental dynamic identifications tests performed; Section 4 illustrates the step-by-step modeling approach adopted to arrive to a numerical model representative of the actual construction; Section 5 includes the results of the seismic assessment; finally, the conclusions of the study are summarized in Section 6.

2. The Basilica of San Sebastian

2.1 Historical Context

The first church of the San Sebastian, made of wood, was built in 1621 on land donated to the Religious Order of the Augustinian Recollects.. The church was inaugurated on the 5th of May in 1621, and was described by historians and story-tellers as “curious”, “well built”, and of “medium” size [11]. During the second *Sangley*[1] rebellion in 1639, the church was looted and damaged by fire. Some years later, in 1645, a devastating earthquake, known as the Luzon earthquake, destroyed the church.After the earthquake, the Recollect monks demolished what was left of the church and started to build a larger church on the same site, this time made of masonry. This second church proved to be more resistant than the previous, lasting for at least ten major earthquakes. From 1859 to 1861 the church underwent extensive renovation and expansion, which added two rows of columns in the center of the nave and raised the height of the roof. Just two years after the renovation works, another devastating earthquake occurred in Manila, causing major damage to the San Sebastian church; leading to its demolition [11]. Once again, the Recollects wasted no time, and started to rebuild a new church.The third version of the church was constructed with wood, in the hope that would be more resilient to earthquakes. It was opened to public on the 20th of January in 1867 and lasted for 13 years, before being severely damaged by the earthquake of 1880. The seismic event caused damage mainly to the walls, but it was found that the timber members were also severely attacked by termites and weevils. The damage was so much that the Head of Civil Works for the Colonial Government of Spain, Genaro Palacios, had no other choice but to condemn the building as a life safety issue.

After losing three buildings due to seismic events, the monks started looking for an earthquake-resistant solution. Palacios, who was also an engineer specialized in seismic engineering, undertook the responsibility of the design, proposing that the new church should be built with metal. He claimed that the new steel church would be stronger, and at the same time lighter than masonry, making it “ideal for

[1] An archaic term used to describe and classify a person of mixed Chinese and Filipino ancestry.

tremors". Overall, it was assumed that the new structure would be "earthquake proof, termite proof, and fire proof".

The design of the building was the result of a close collaboration between Palacios and the Recollect monks from Manila and Madrid, and lasted for three years. The final design consisted of a prefabricated steel Roman Catholic Basilica, with a fusion of baroque and neo-gothic architectural styles. By the time the design was finished, a bid concerning the steel production started and was issued to companies in Spain, England, France and Belgium. The bid was won by the Belgian company *Société Anonyme de Travaux Publics*, that was known for working on many large-scale structural steel constructions, such as the *Museo Nacional de Ciencias Naturales*, in Madrid, Spain.

Before shipping the steel to Philippines, a mock-up was constructed in Belgium by the company (Figure 1). Moreover, the pieces were already primed, firstly with a red lead in linseed oil, and then with a white lead in oil pant, ready to receive the decorative trompe l'oeil finish locally. Furthermore, the columns were pre-assembled with all sides fully riveted, ready to be stacked and spliced together on site. The impressive amount of 1,500 tons of steel and cast iron elements, along with the stained glass, arrived in Quiapo, Manila between June 1888 and August 1890.

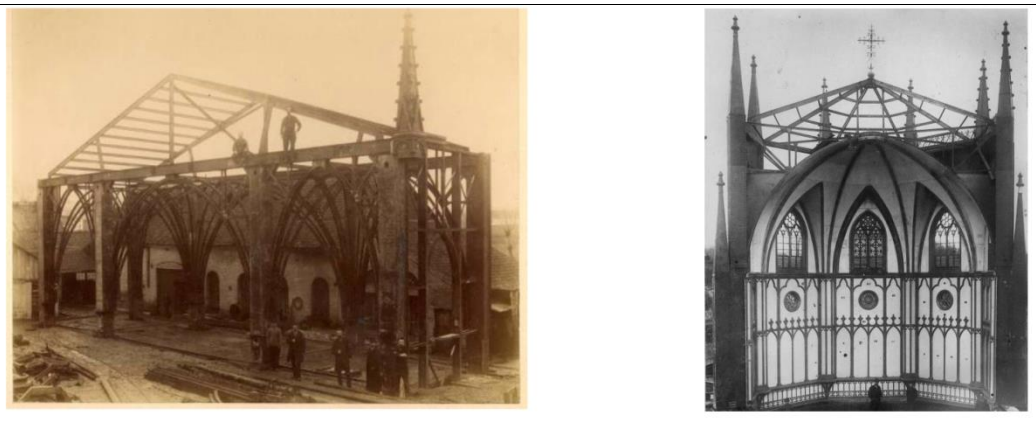

Figure 1. Trial assembly of (a) a part of the nave and (b) the dome before shipping from Belgium. Obtained from [10].

The construction was carried out by local workers, artisans and craftsmen, and supervised by Belgian engineers. All prefabricated elements were screwed, bolted and riveted on-site. In order to hide the industrial nature of the building, the structural elements and connections were covered by moldings, cornices, flouting and other decorative details. Similarly, the seams and joints were filled with putty so as to hide the appearance of the steel. The final surfaces were faux finished to look like stones. Due to a storm that capsized one of the ships going to Manila, the prefabricated steel reredos (a screen or decoration behind the altar) was lost. Consequently, a wooden altar was built locally as replacement. Figure 2 shows a historical photo of the construction phase.

Figure 2. Construction of the Basilica on-site in Quiapo, Manila. Obtained from [10].

The construction works lasted a decade, and on August 15, 1891, the new steel church was inaugurated. Pope Leo XIII declared the church as a Basilica in 1890, one year before its completion. To this day, the San Sebastian Basilica has survived 11 major earthquakes and remains the only surviving neo-gothic church from the Spanish colonial era in the Philippines. A general view of the current state of the church is shown in Figure 3.

Figure 3. Photo of the present San Sebastian Basilica.

2.2 Description of the Structure

In plan, the Basilica is extended in a typical rectangular shape with dimensions of 25 m wide and 53 m long, and maintains symmetry about the longitudinal axis (Figure 4). Two bell towers exist in the facade with a height of 48 m, while a dome with diameter of 10 m is protruding above the central nave. The interior space of the church is composed of a nave, a chancel and a choir loft (Figure 5). The structural system of the Basilica consists of hollow steel columns, braced vertically with steel angles. At the top, the ceiling is suspended by a truss system and a separate roof framing is resting on the top of the columns. Since the initial design is an attempt to mimic masonry gothic architecture, the peripheral walls and the ceiling is covered by thin steel plate panels that are connected to the steel framing system. A more detailed description of the different structural parts follows.

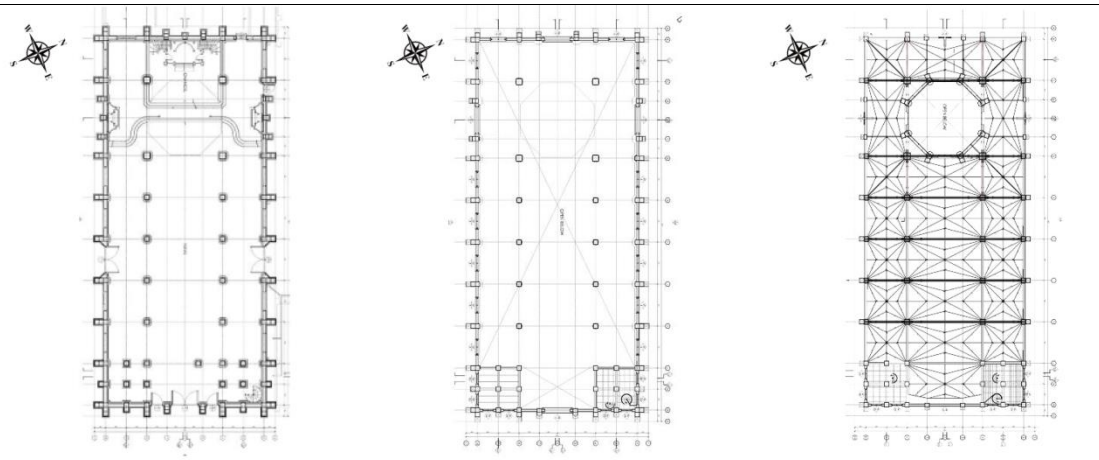

Figure 4. (a) Foundation, (b) second floor, and (c) roof level plan of the Basilica.

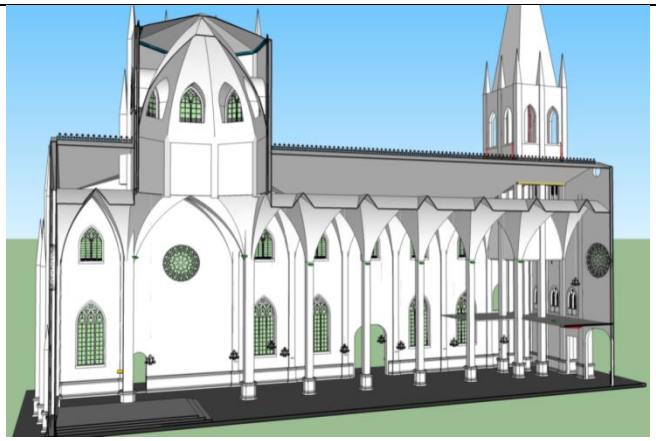

Figure 5. Section of a 3d model of the Basilica. [10]

The foundation system consists of concrete rectangular footings, which are connected by concrete tie beams forming a grid in plan. The columns bear on steel base plates, which are bolted into the footings; around 2.3 m bellow the ground-floor level. Moreover, another grid of tie beams, made of steel, exist just below the ground floor level. Figure 6 depicts the basic components of the foundation system. Due to the dense presence of columns at the base of the towers, a continuous concrete foundation has been constructed locally. Overall, the foundation system of the church can be considered adequately stiff, given the significant lever arm provided by the double tying grid. Moreover, it is worth to note that since the Basilica was built over the foundations of the previous churches, enhanced stability and reduced soil settlement phenomena are expected to characterize the site.

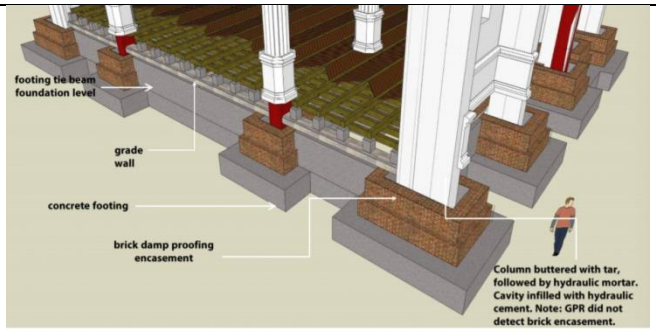

Figure 6. 3D representation of the foundations system of the Basilica. [10]

The Basilica has 65 columns made of Rectangular Hollow Sections (RHS). The most common column dimension is 600x600 mm, with the exception of the four columns supporting the dome that are slightly larger with a section 800x800 mm, and some narrower columns that flank the rose window with 600x400 mm section. Each column has been constructed by four steel plates of 5mm thickness, connected at the corners by angle bars of 5mm thickness and rivets (Figure 7). As already mentioned, the column were assembled in Belgium and delivered in segments of 6m, which were spliced together on the site. In some areas on the exterior of the Basilica, a series of up to five RHS columns were connected by steel plates, creating buttressed columns.

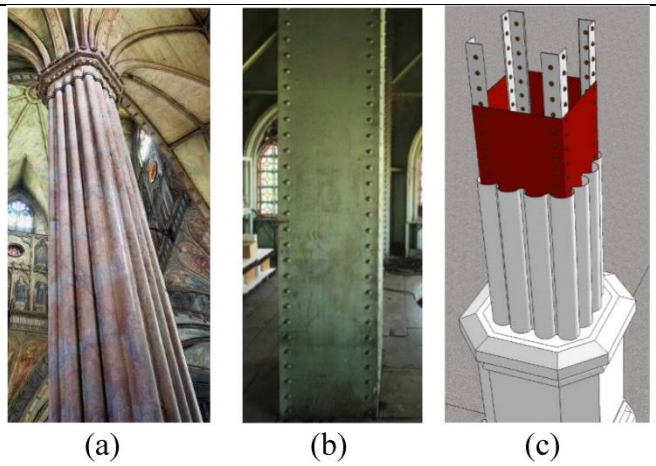

Figure 7. Photo of (a) an internal decorated column, and (b) an internal unexposed column. (c) 3D representation of a typical column configuration. [10]

Along the perimeter of the plan, the different columns are connected by cross bracings and a framing system of I-members (Figure 8). This framing and bracing system is absent at the areas of openings, loosing therefore its continuity across the height. Moreover, in order to hide the bracing system and mimic the neo-gothic masonry architecture, steel plates of 3 mm thickness were introduced; creating therefore cavity walls. In the attic and the towers, where the access was not allowed to the pilgrims, only one leaf of steel plates was placed. Those steel plate panels have dimensions of around 1.5x2 m and are connected to the rest structural components with angle bars.

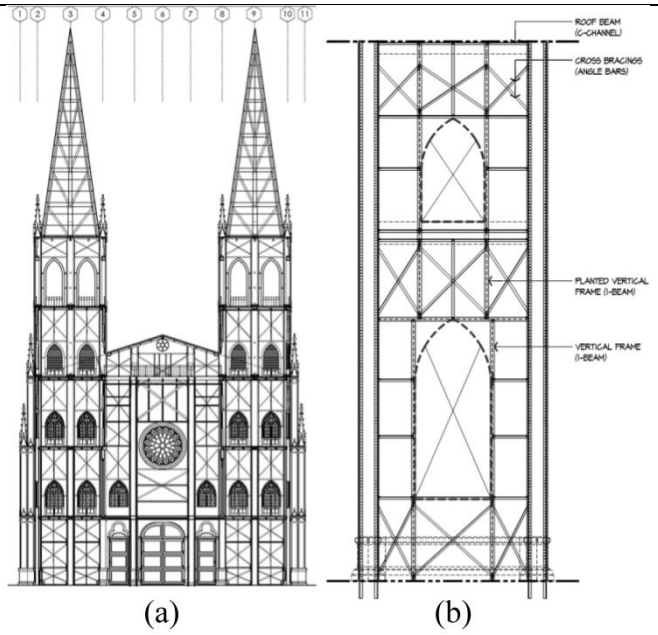

Figure 8. The cross-bracing and framing system of (a) the façade, and (b) a typical bay of the peripheral walls. [10]

The suspended ceiling replicates the architectural morphology of masonry rib vaults. The ribs are composed by curved I-beams, while the space in-between is covered by steel plates of 3mm. In more detail, the section of the I-beam ribs has an additional flange in the center of the height, in order to fasten on it the steel plates, while moldings that replicate the masonry ribs are fastened at the lowest flange. The ribs that connect the columns in the plan grid (in equivalence, the arches of a masonry vault) are composed by two parallel I-beams, while a truss system above the ceiling is connecting the columns, providing additional stiffness.

A typical roof truss system of I-beams is resting upon the top of the external columns, while being separate from the ceiling. Purlins bridge the trusses, upon which hot-dipped galvanized sheets rest, composing the final roofing. In order to provide additional stability to the trusses out-of-plane, four central parallel trusses are cross-braced in the longitudinal direction.

The central dome has an octagonal configuration, constituted with columns at each corner and openings between consecutive columns. The bottom half of the columns is buttressed with double sections of 600x600 mm, and reduced into single sections in the top half. Finally, the walls below the openings are crossed braced, providing additional stiffness.

The towers have four floor levels and belfries with spires on top (Figure 8a). The flooring system is composed by steel beams with timber finishes, except for last one on the top that is made of 0.1m thickness concrete slab, The spires are composed by four corner leaning columns (hip rafters), one central column, purlins and diagonal cross braces that connect the central column with the hip rafters (Figure 9a). The cross section of the central and the corner columns decrease across the height of the spire, while at the final top part the central column is absent and horizontal cross braces tie together the corner columns (Figure 9b).

(a)

(b)

Figure 9. Photo of the (a) lower part, and (b) upper part of the farming system of the spires.

At the north side of the Basilica exists the convent building made of reinforced concrete. The building was erected in the 1950s and has four floors The convent appears to be in alignment with the first three buttressed columns along the east side of the north wall of the Basilica. Unfortunately, the exact gap (or contact) of the two structures cannot be examined due to difficulties of access. Despite the very close distance between the two structures, no pounding damage has been observed by now.

3. Investigation and Dynamic Identification

3.1 Investigation and Diagnosis

Since its founding, the Save San Sebastian Conservation and Development Inc. has conducted an extensive investigation and diagnosis campaign of the Basilica. This includes numerous tests and methods, briefly described below, while the interested reader is referred to [10] for further details.

A visual assessment was carried out, including the use of endoscopic investigation to gain access in the cavity of the columns and the walls. This highlighted the presence of retained water at the base of 24 columns, which is probably leaking from the roof top. In addition to visual inspection, a three-dimensional laser scanning was carried out, both at the interior and exterior of the Basilica. The exact geometry of the point cloud was then analyzed and geometrical imperfections or defects could be recognized (Figure 10). More specifically, the drift of the columns was observed within allowable levels, while bulging of some parts of the walls at the corner were also recognized, caused by a previous seismic activity or occurring during construction. It is worth noting that in this work the geometrical data obtained using the laser scanning have been analyzed per se, as the decorative elements of the Basilica do not allow a straightforward automatic "point cloud to structural analysis" procedure (e.g. see [12], [13], [14]).

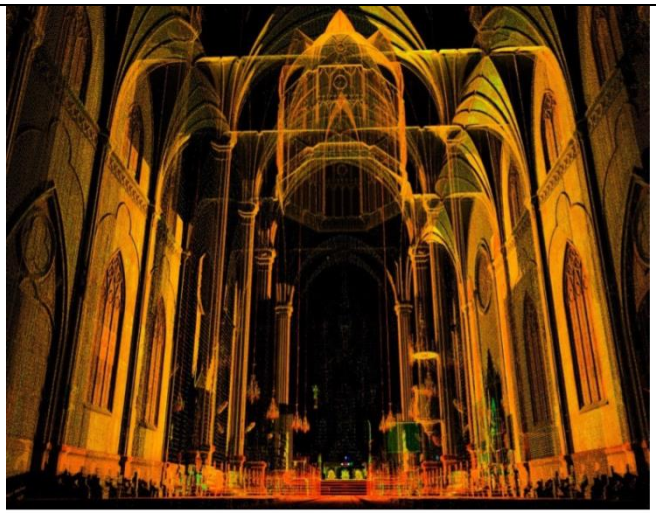

Figure 10. Point cloud data of the interior of the Basilica. Obtained from [10].

Concerning the steel, both chemical and mechanical tests were conducted. A wet chemical metallurgical analysis showed that the Basilica is made of mild steel, resulting in high corrosion resistance, ductile response and weldability. The mechanical tests made presented an average yield and ultimate strength of 325 MPa and 376 MPa, respectively. The condition of the material against corrosion was also assessed. Paint impedance tests recognized the areas of the Basilica where the paint is still acting as protection against corrosion and the areas that are unprotected.

Furthermore, the cross sectional losses due to corrosion were measured using both a caliper and ultrasonic thickness gauging. The conclusion was that there is an average material loss of 10%. It should be noted that especially for the columns this percentage increases to 23% due to the leaking water mentioned before, while in five columns this percentage raises locally up to 76% (Figure 11).

Figure 11. Retained water and severe damage due to corrosion at the base of a corner column. Obtained from [10].

The sub-ground and soil conditions were also examined. Ground penetration radar (GPR) was employed to scan the whole plan of the Basilica, while three floor inspection pits were also opened. The GPR scan verified the presence of the tie-beams and identified concentration of water beneath the spires. Furthermore, soil tests were realized in order to recognize the soil type and the level of groundwater. Specifically, the groundwater was measured just 1.5 m below the floor level with a seasonal variation of 0.6 m, while the soil type was identified as argillaceous.

Finally, a recording system of temperature and relative humidity was installed in order to monitor the environmental conditions of the Basilica. In fact, the high climatic variations of Philippines might lead to water infiltration or accelerate surface corrosion phenomena.

3.2 Dynamic Identification Tests

The aim of the dynamic identification tests was to estimate the main dynamic properties of the structure, namely the frequencies, the mode shapes and the

damping ratios. University of Minho carried out dynamic identification tests at the San Sebastian Basilica in April of 2016, using an output-only technique. This technique records and processes data of ambient vibration that act on the structure at service conditions, such as wind and traffic. The instrumentation that was used to perform the tests consists of twelve piezoelectric accelerometers (with sensitivity of 10 V/g, frequency range from 0.15 to 1000 Hz, and dynamic range of ±0.5 g), coaxial cables and a 24-bits data acquisition system.

Fifty-one positions of the structure were chosen to place the accelerometers, at which the highest modal displacements were expected. Only horizontal degrees of freedom were selected and recorded, distributed at the top of the external walls, the dome and the bell towers. Figure 12 shows the exact locations of the accelerometers set-up. One degree of freedom, at the center of the nave, was kept as reference (Figure 12a), and the position of the rest of the accelerometers was changed, resulting in seventeen different setup configurations. In each configuration, 30 minutes of ambient vibration were recorded at 200 Hz sampling rate.

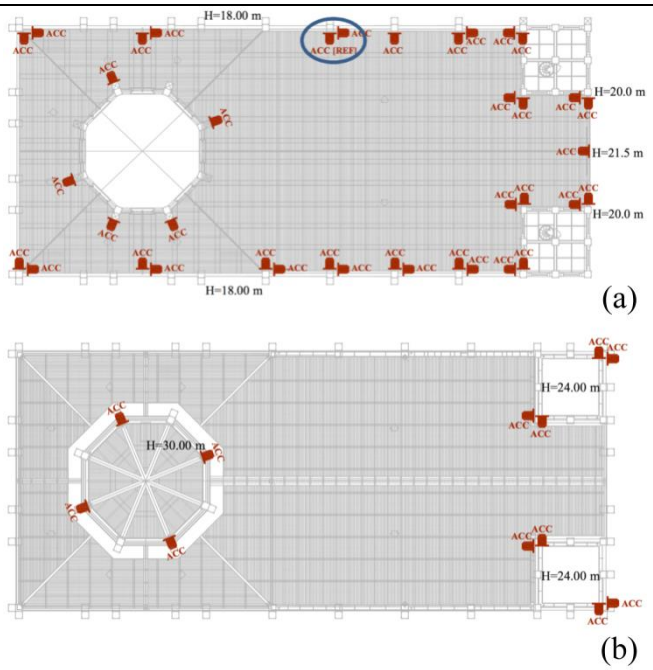

Figure 12. Set-up of the accelerometers at (a) the roof level, and (b) the dome and towers level.

Two well-established methods, both in frequency and time domains, were employed to estimate the dynamic properties of the church using the ARTeMIS software [15], namely: a) the Enhanced Frequency Domain Decomposition (EFDD); and b) the Stochastic Subspace Identification Principal Component (SSI-PC) [16]. Six modes were estimated in the range of frequency of 2.53 Hz – 5.81 Hz (Figure 13) and the results are reported in Table 1. Here, MAC indicates the Modal Assurance Criterion (MAC) value [16], discussed below. More specifically, Figure 13 depicts the singular values of the cross-power spectral density matrices of all the setups for the EFDD method [16], where the pick-peaking method is used to identify the modes.

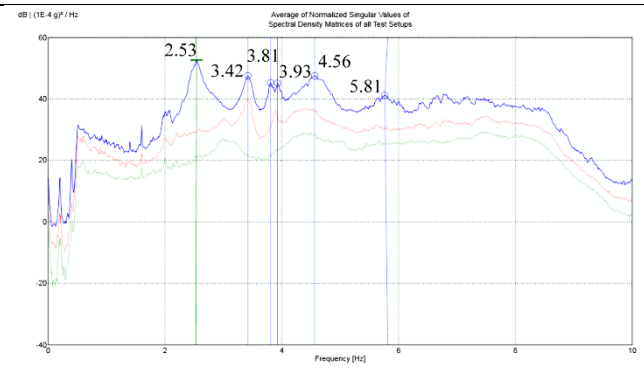

Figure 13. Average of normalized singular values of the spectral density matrices of all test setups (EFDD method). The six identified modes are highlighted.

Table 1. Experimental dynamic properties obtained using the EFDD and SSI-PC methods.

Mode	EFDD		SSI-PC		$\Delta_{Freq.}$ [%]	MAC
	Freq. [Hz]	Damp. [%]	Freq. [Hz]	Damp. [%]		
1	2.53	2.6	2.53	2.5	0.2	0.996
2	3.42	-	3.43	1.7	0.2	0.388
3	3.81	-	3.86	2.3	1.3	0.606
4	3.93	-	3.95	2.0	0.6	0.659
5	4.56	-	4.57	3.1	0.3	0.812
6	5.81	1.2	5.78	4.4	0.6	0.715

Figure 14 presents the estimated mode shapes using the EFDD and SSI-PC methods. The first mode (2.53/2.53 Hz) corresponds to the first global mode in the transversal direction of the Basilica. In this mode, the longitudinal walls present a single curvature in plan. The second mode (3.42/3.43 Hz) represents a local mode of the east bell tower, which corresponds to a torsional/wrapping mode of the tower, distorting its cross section. Such modes usually appear to be stiffer than the bending modes, while it should be noted that due to the convent building and the existence of damage, the Basilica might possess an asymmetric dynamic behavior. Mode three (3.81/3.86 Hz) indicates the bending mode of the bell towers in the longitudinal direction. In this mode, the bell towers are out-of-phase. The fourth mode (3.93/3.95 Hz) is the bending mode of the bell towers in transversal direction. Finally, the fifth (4.56/4.57 Hz) and the sixth (5.81/5.78 Hz) modes correspond to the second and third global mode of the Basilica in the transversal direction, with second and third curvature of the longitudinal walls, respectively. In both modes, the bell towers are in-phase. Using the EFDD method, the damping ratios were estimated only for the first and sixth mode with values 2.6% and 1.2%, respectively.

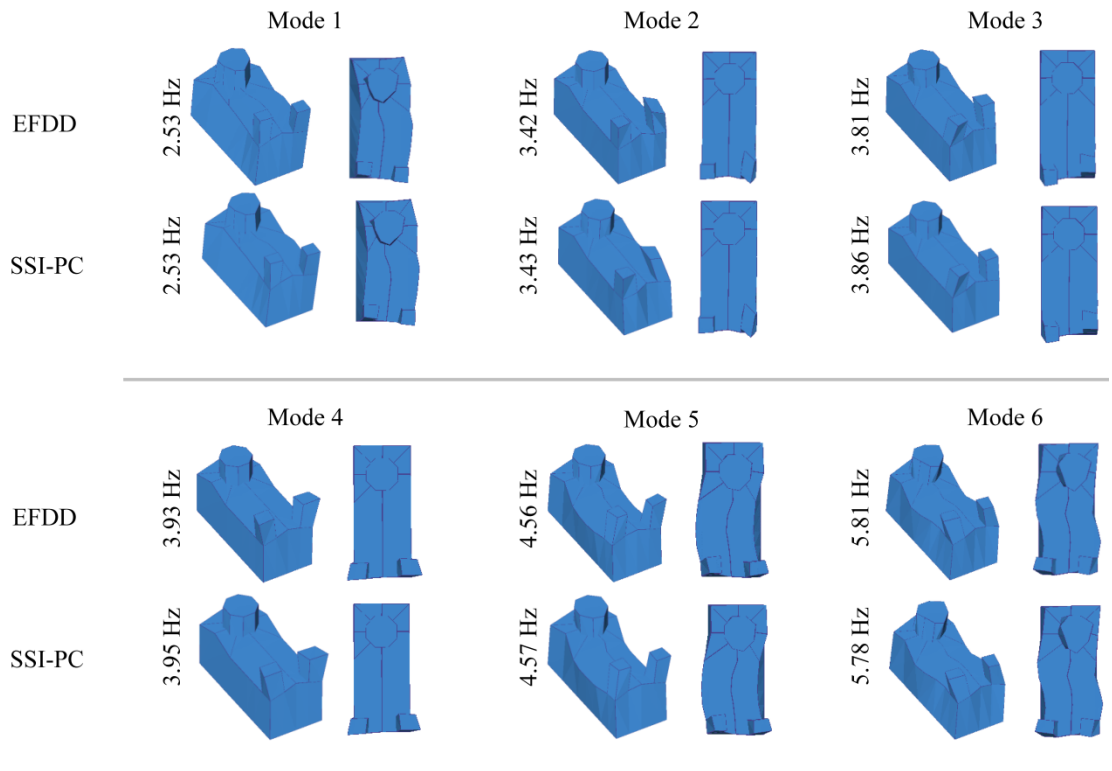

Figure 14. Experimental mode shapes of the Basilica, estimated using the EFDD and SSI-PC methods.

The SSI-PC method yielded almost identical modes in terms of frequencies (Table 1). The difference between the natural frequencies obtained by the two methods is less than 2%. Similarly, the mode shapes were also indicating the same response: a) the modes 1, 5 and 6 represented the first, second and third global modes in the transversal direction; b) modes 2, 3 and 4 correspond to local modes of the bell tower. Moreover, using the SSI-PC method the damping ratios were estimated for all modes and are shown in Table 1, ranging from 1.7% to 4.4%. It should be mentioned that low values of damping ratio are commonly obtained when output-only techniques are used for dynamic identification tests [17].

A quantitative comparison of the mode shapes of the two methods was performed based on the MAC values [16] and is presented in Table 1. A MAC value of 1 means there is perfect correlation between the two eigenvectors of the mode shapes, whereas a value close to zero indicates the absence of correlation. The average of the MAC values for all mode shapes is equal to 0.70, in which the lowest MAC value is equal to 0.39 for the second mode. This low MAC value indicates that

either some setup configurations failed to obtain this mode with the SSI-PC method or the mode does not exist. The global transversal modes (1, 5 and 6) of the Basilica present an average MAC value equal to 0.84, which indicates a rather good match between the modes estimated through the EFDD and SSI-PC methods.

4. Numerical Model of the Basilica

The outcomes of the extensive investigation campaign and dynamic identification tests were afterwards integrated into a Finite Element (FE) numerical model of the Basilica. More specifically, the Midas FX+ Customized Pre/Post processor was utilized, while the analyses were conducted using the DIANA FEA software [18],[19]. Importantly, the model preparation and calibration process included the following methodological phases: 1) a step-by-step procedure to arrive from a simple to a more detailed model, and 2) a model updating procedure, in order to match the modal characteristics with the experimental dynamic identification tests. A thorough description of these phases follows, prior to the utilization of the model in order to assess the seismic safety of the Basilica.

4.1 A Step-by-step Modeling Approach

The modern computational capabilities and developments have provided engineers with powerful structural analysis tools. However, such tools require knowledge of how to use them and the adoption of realistic input values. These aspects play a key role in a structural design or assessment procedure, as the analysis might end-up governing the procedure, instead of assisting it. This is especially crucial for cultural heritage structures, such as the Basilica, since a non-realistic assessment procedure (even if it is sophisticated) might either lead to inadequate interventions, compromising the safety of the monument, or lead to extensive retrofitting solutions, wearing out its authenticity.

A step-by-step process was adopted in the modeling of the Basilica, in order to control key characteristics through the path of simplicity to sophistication. This strategy is essential because the structural system of the Basilica is unique and quite complex. More specifically, five models were constructed, starting from a simple

model, where only the main structural members were considered, and arriving to a complex model, where all the structural members were simulated, including the secondary ones, together with their damage.

All the models adopted the elastic material parameters shown in Table 2. It should be noted that whenever some elements were not modeled explicitly, their mass was calculated and assigned to the modeled elements, normalizing artificially the total mass by increasing the density. The mesh size of the beam elements was set approximately equal to the height of their cross-section, while when shell elements were present (as in models 4 and 5), the mesh size was set around 0.5 m for the dome and 0.3 m for the walls and vaulting.

Table 2. Adopted elastic material properties of the models.

Property	Parameter & Units	Value
Material density	ρ [kg/m^3]	7850
Modulus of elasticity	E [GPa]	200
Poisson's ratio	ν	0.30

Each model was verified in the elastic field for consistency and was compared with the other models and the experimental dynamic identification tests, which represent the actual construction. The consistency of each model was verified by performing a self-weight analysis in order to compare the total weight of the structure and some key nodes' displacements. The comparison of each model with the rest of the models and the experimental tests is shown in Figure 15 and Table 3, in terms of frequencies and mode shapes, using the MAC values and having as reference the experimental results. It is noted that the consistency verification is not presented here, but the self-weight is the same for all the models (see [20] for details).

The first model included the columns, the roof members, the towers, the dome, the cross braces and the framing system of the walls, and the truss system above the ceiling (Figure 15). All the members were set as CL18B three-node three-

dimensional beam elements [19], which are based on the Mindlin-Reissner theory and include shear deformation. The cross-sections of the beam elements were either chosen by the built-in options of FX+ Midas or defined manually using an arbitrary cross section. The base of the columns was set at the foundation level (2.3 m bellow the ground level) and fixed. This can be considered a reasonable simplification, since two parallel grids of tie-beams exist, providing a very high rotational stiffness to the foundation system. In total, the model included 54,905 beam elements and 645,198 degrees-of-freedom (DOF).

By comparing the results (Figure 15 and Table 3), firstly it appears that the numerical model cannot replicate the second mode, which corresponds to the torsional/wrapping distortion of the cross section of the east tower. This mode (if it actually exists) is attributed to possible local deficiencies of the diaphragms of the tower, such as an inefficient or damaged connection, given its wrapping shape. Nevertheless, such deficiencies are unknown and not included in the model, and thus, none of the numerical models could identify this mode. By comparing the model 1 with the experimental test, a small correlation can be observed. Firstly, the model appears to be too flexible, especially for higher modes. In terms of mode shapes, a medium correlation has been obtained for the first mode, as the dome is not participating in the response. Better results can be observed for the third mode, where the model seems capable in reproducing the first bending mode of the towers in the longitudinal direction, despite having some bias of transversal movement. The rest of the modes are purely replicated.

The second model was built on the previous model, by adding the primary ribs of the vault that span between the columns, as beam elements, similarly. This model included 57,552 beam elements and 673,920 DOF (Figure 15). The results of model 2 shows a similar bad correlation, while only the first mode progresses. For this case, the stiffness has a significant gain, indicating the importance of the main ribs.

The third model improved over the second by introducing all the ribs of the vaulting system. The model included 69,254 beam elements and 881,038 DOF

(Figure 15). It appears that model 3 improves significantly the third and the fourth mode, related to the towers, both in terms of frequencies and mode shapes. At the same time, the fifth mode is also improved, but mainly in terms of response. Nevertheless, this model does not provide the same accuracy on the first mode, as the model 2.

Model four completed the ceiling system by adding the steel plate panels (Figure 15). These elements were modeled using curved shell elements CQ40S and CT30S, which are eight-node shell elements based on the Mindlin-Reissner theory [19]. The model was composed by 59,587 beam elements, 19,605 shell elements and more than 771,885 DOF. Model 4 highlights a great improvement in the stiffness of the global modes (modes 1, 5 and 6). This outcome underlines that although curved and thin, the ceiling plays a key role in the global response as a deformable diaphragm. Despite that, a bad correlation is maintained for the local modes of the towers.

The fifth model was the most elaborated and introduced: a) the steel plate walls, b) the stiffness of the framing around the openings of the towers through equivalent braces, c) the floor beams of the towers, d) the concrete floor of the towers using equivalent rigid bracing, and e) lateral springs to account for the presence of the neighboring convent building (Figure 15). In more detail, the single leaf steel plate walls were simulated with the shell elements CQ40S and CT30S. The double leaf steel plate walls were modeled with the layered shell elements CQ40L and CT30L. These are similarly eight-node shell elements based on the Mindlin-Reissner theory; however, different materials can be set through the thickness, as distinct layers. Therefore, the complete cavity panel could be simulated by two external layers and an intermediate layer with zero mass and modulus of elasticity, providing the appropriate lever arm and thus stiffness. This modeling strategy includes the assumption of strain compatibility through the thickness. Since the structure has a dense framing system that connects the two sides also exists, this assumption was accepted for simplicity. Alternatively, the actual cross section of the cavity walls could be modeled explicitly by using two separate shell elements in parallel across the thickness, and thus eliminating the aforementioned assumption.

Nevertheless, such an option would increase significantly the DOF used (doubled for the shell elements), and therefore the layered elements were deemed as a good compromise between sophistication and simplicity. The windows of the towers have a small framing system, in order to replicate the pointed arches of gothic architecture. The stiffness of this system was evaluated using a local model, and an equivalent bracing system of beam elements was introduced at the position of the openings. Similarly, the concrete floor of the towers was represented by a rigid bracing system of beam elements. Furthermore, the rest of the floors were modeled using beam elements explicitly for each beam of the floors. Finally, nine lateral springs were placed over the wall that is seemingly in contact with the convent building, replicating its stiffness. The model was composed by 56,452 beam elements, 50,555 shell elements and more than 1,021,940 DOF.

Model 5 appears to overestimate the stiffness of the Basilica, in contrast with all the previous models that were mainly underestimating it. The stiffness has been increased due to the walls for the case of the global modes, and mainly due to opening frames for the case of the local modes. Nevertheless, the mode shapes match improved with the dynamic identification test, indicating a good potential for model 5.

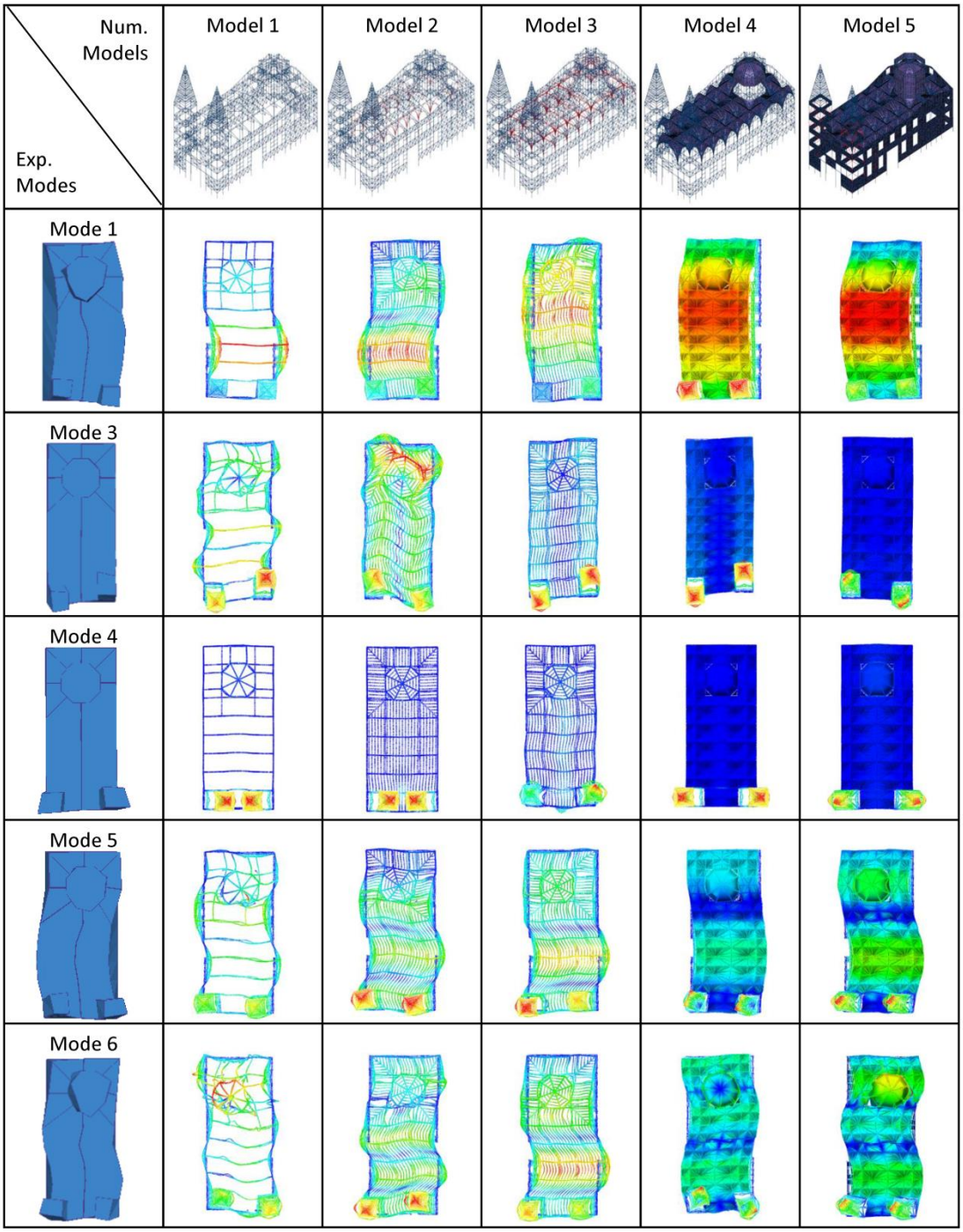

Figure 15. Comparison of experimental and numerical mode shapes.

Table 3. Comparison of the natural frequencies and the MAC values of the experimental results and the numerical models.

Exp. Results	Model 1			Model 2			Model 3		
	Freq. [Hz]	Error [%]	MAC	Freq. [Hz]	Error [%]	MAC	Freq. [Hz]	Error [%]	MAC
2.53	2.22	-12	0.64	2.38	-6	0.75	2.26	-11	0.67
3.81	3.14	-18	0.89	2.59	-32	0.70	3.15	-17	0.87
3.93	3.22	-18	0.51	3.22	-18	0.48	4.41	12	0.74
4.56	2.80	-39	0.57	2.80	-39	0.58	3.01	-34	0.81
5.81	3.34	-43	0.57	3.40	-41	0.52	3.01	-48	0.65
Ave.	-	26	0.64	-	27	0.61	-	24	0.75

Exp. Results	Model 4			Model 5 (before calibration)		
	Freq. [Hz]	Error [%]	MAC	Freq. [Hz]	Error [%]	MAC
2.53	2.57	2	0.84	2.9	15	0.78
3.81	3.17	-17	0.83	4.77	25	0.82
3.93	3.22	-18	0.48	5.08	29	0.55
4.56	4.2	-8	0.79	5.11	12	0.84
5.81	5.13	-12	0.58	6.05	4	0.63
Ave.	-	11	0.70	-	17	0.72

The outcomes of the step-by-step modeling approach indicate that the “actual” response, as observed by the dynamic identification tests, lays close to the response of the models four and five. At this point, it is clear that any further effort to obtain a more accurate model should explore the inherent assumptions of those two models. An attempt to enumerate the main assumptions follows: 1) the models assume rigid connections between the different members, 2) the models disregard any presence of damage due to corrosion, 3) soil-structure interaction is not taken

into account, 4) the effect of contact of the convent building is not clear by the investigation and 5) some masses may be lacking in the model (e.g. equipment, bells etc.). The first assumption was made since the Basilica's connections are riveted. In general, such connections are not expected to allow movement due to the closure of the diameter clearance during the application process, and due to the active clamping forces [21], [22] [23]. The second assumption was made for simplicity, since only a small percentage of 10% material loss, on average, was found (see Section 3.1 Investigation and Diagnosis). The assumption to neglect soil-structure interaction was made due to two main facts: a) the Basilica stands on the same site of the three previous churches, and therefore the soil had been compacted, and b) two separate grids of tie beams exist at the foundation level, providing significant rotational stiffness at the foundations. The fourth assumption was taken into account by nine springs with simple geometrical considerations, although the in-situ investigation could not verify if the two structures are actually in contact, due to difficulties in access. Finally, any disregarded operational masses were not expected to be a significant proportion of the total mass of the construction, and therefore could be neglected.

Nevertheless, the aforementioned five assumptions have all a common influence on the numerical model: to make it stiffer than the actual construction. Therefore, it is apparent that it is the fifth model that should be manipulated in order to minimize the influence of those assumptions, and arrive to a more flexible model. Such an attempt follows next.

4.2 Model Updating

A model updating procedure was followed in order to obtain a model that replicates better the actual structure. The parameters to vary should be defined in a rational way, so to not lose control over the model. The previous Section indicated five assumptions that may hinder the model to match the experimental tests results. Next, the second and the fourth assumptions are examined explicitly, while the first assumption is examined implicitly.

Concerning the second assumption, the material loss due to corrosion was significantly higher for the columns (23% in average), when compared to the rest of the structure (10% in average), while a rather high percentage of 73% was observed in five columns. Therefore, the damage of the columns due to corrosion should be taken into account. From a phenomenological point of view, the corrosion is inducing a decrease on the effective section of the members [24], and therefore the modeling approach should reduce the sections of the finite elements. However, the model updating procedure requires several different models to be analyzed, and since all the sections of the 65 columns are defined manually as arbitrary sections, such process would be highly time consuming. As a result, the modulus of elasticity of the columns is chosen to vary, as an equivalent simplification, instead of the cross-sectional loss.

Furthermore, model 5 showed that the walls of the Basilica increase significantly the stiffness of the structure, where their thickness was assumed 3 mm per leaf, according to the original design. Due to its influence, this thickness should also be reduced by the damage of corrosion. As a result, the thickness of the walls is chosen to be the second parameter to vary in the model updating procedure. It is of interest to note here that the variation of the thickness of the walls can be seen also as an implicit consideration of their rigidity. Since their initial conception was to mimic the masonry architecture, those elements were used as “secondary”, and therefore their connections may have not been treated with the same care.

Finally, the influence of the convent building can be calibrated by varying the stiffness assigned to the respective springs. The model updating method proposed by [25] and successfully applied by several authors e.g. [26], [27], [28] was adopted, in which the frequency i of the numerical model ${f_i}^N$ can be estimated by :

$$ {f_i}^N(X_1, X_2, \dots, X_n) = C_i + \sum_{k=1}^{n} [A_{ik} X_k + B_{ik} (X_k)^2] \qquad (1) $$

where X_k $(k = 1,2, \dots, n)$ are the variables to calibrate and A_{ik}, B_{ik} and C_i are constants. The $(2n+1)$ constants can be obtained by the following system of equations:

$$
\begin{aligned}
f_i^N(X^B{}_1, X^B{}_2, \dots, X^B{}_n) &= C_i + \sum_{k=1}^{n} [A_{ik} X^B{}_k + B_{ik} (X^B{}_k)^2] \\
f_i^N(X^L{}_1, X^B{}_2, \dots, X^B{}_n) &= C_i + \sum_{k=1}^{n} [A_{ik} X^L{}_k + B_{ik} (X^B{}_k)^2] \\
f_i^N(X^U{}_1, X^B{}_2, \dots, X^B{}_n) &= C_i + \sum_{k=1}^{n} [A_{ik} X^U{}_k + B_{ik} (X^B{}_k)^2] \\
&\dots \\
f_i^N(X^B{}_1, X^B{}_2, \dots, X^L{}_n) &= C_i + \sum_{k=1}^{n} [A_{ik} X^L{}_k + B_{ik} (X^L{}_k)^2] \\
f_i^N(X^B{}_1, X^B{}_2, \dots, X^U{}_n) &= C_i + \sum_{k=1}^{n} [A_{ik} X^U{}_k + B_{ik} (X^U{}_k)^2]
\end{aligned}
\tag{2}
$$

where $X^B{}_k$ represents the base values of the calibration variables. The variables $X^L{}_k$ and $X^U{}_k$ represent the lower and upper limit values respectively. The upper limit is chosen to be the value used in the previous model 5, and the lower limit is chosen by assuming a reasonable reduction, and the base value somewhere in between these two.

A least square minimization of the difference between the numerical frequencies f_i^N and the experimental frequencies f_i^E is performed after calculating the constants as follows:

$$
\begin{aligned}
\pi &= \sum_{i=1}^{m} w_i {\varepsilon_i}^2 \\
\varepsilon_i &= f_i^E - f_i^N(X_1, X_2, \dots, X_n)
\end{aligned}
\tag{3}
$$

where π is the objective function, ε is the residual function, w is the weight constants, and m is the number of frequencies considered.

The base, lower limit (LL), and upper limit (UL) values adopted are presented in Table 4:

Table 4. Calibration variables of the first attempt.

Element	Parameter	Units	Base	LL	UL
Columns	E	GPa	150	50	200
Walls	t / leaf	mm	2	1	3
Springs	k	N/m	50 000	0.0001	100 000

The model updating procedure was performed for two schemes. In the first scheme, all the experimental modes (excluding the second experimental mode) were considered as reference f_i^E, and in the second scheme only the global modes (1st, 5th and 6th) were considered are reference. The variable parameters were then derived as illustrated in Table 5.

Table 5. Obtained values of the first calibration attempt.

Element	Parameter	Units	Modal Updating	
			Scheme 1: 5 Modes	Scheme 2: 3 Modes
Columns	E	GPa	65.58	85.27
Walls	t / leaf	mm	1.98	1.15
Springs	k	N/m	2451.24	0.0001

Then, the employment of those values to model 5 derived the modal results shown in the first columns of Table 6**Error! Reference source not found.**. By observing the results of this attempt, it appears that both model updating schemes provide a much better estimate of response, both in terms of frequencies and mode shapes. Nevertheless, it is also highlighted that the calibration according to the second scheme is superior. This is attributed to the fact that global modes are leading the process. Moreover, since the estimation of the springs' stiffness was

minimized in the first scheme, another attempt followed, excluding the springs, and removing them from the model. The results of method are then shown in Table 7.

Table 6. Comparison of the natural frequencies and the MAC values of the experimental results and the calibrated models.

Exp. Results	Model 5 (1st attempt, scheme 1)			Model 5 (1st attempt, scheme 2)			Model 5 (2nd attempt, scheme 2)		
	Freq. [Hz]	Error [%]	MAC	Freq. [Hz]	Error [%]	MAC	Freq. [Hz]	Error [%]	MAC
2.53	2.62	4	0.62	2.50	-1	0.80	2.54	0	0.84
3.81	3.44	-10	0.53	3.98	4	0.89	4.04	6	0.87
3.93	4.18	6	0.46	4.41	12	0.48	4.49	14	0.53
4.56	4.78	5	0.70	4.60	1	0.77	4.64	2	0.85
5.81	5.54	-5	0.64	5.53	-5	0.67	5.53	-5	0.69
Ave.	-	6	0.59	-	5	0.72	-	5	0.76

Table 7. Calibrated variables of the second attempt.

Element	**Parameter**	**Units**	**Base**	**Scheme 2: 3 Modes**
Columns	E	GPa	150	91.5
Walls	t / leaf	mm	2	1.08

The outcomes of the model updating procedure show an overall improvement. In more detail, the three global modes (1st, 5th and 6th) are in very good agreement with the experimental tests, both in terms of frequencies and mode shapes. A perfect match in terms of frequency in achieved for the 1st mode, which is also the most important. The local modes of the towers indicate a lower correlation,

especially for the mode 4. Yet, the general view still remains the best fit of all the previous attempts.

The values of the calibrated parameters should also be examined. In this case, 1) the springs that replicate the contact with the convent building were erased; 2) the Modulus of Elasticity of the columns introducing the corrosion damage was set to 91.5 GPa; and 3) the effective thickness of the steel plate walls was defined as 1.08mm. The first point indicates that probably there is no contact between the two structures, and is considered physically acceptable. The second point highlights that the columns are expected to be seriously damaged by corrosion. This outcome is important per se, and indicates that a more extensive investigation or actions are needed about the columns and especially their base, where water is sustained. Furthermore, it seems that it would be specifically interesting to model, individually, the local damage of the five columns that suffer relevant material deterioration. This requires a detailed damage survey with the location of each damage and its severity to be then individually considered in the numerical model. Thus, this work is focused on the global behavior of the structure, considering the existing damage using a simplified method, which is calibrated with respect to the experimental frequencies. i.e. same stiffness. Finally, the effective thickness highlighted by the third point appears realistic, as it is expected to include damage due to corrosion and modeling errors arriving by the rigid connections assumption, at the same time.

5. Seismic Assessment of the Basilica

To conclude about the safety of the Basilica, its seismic capacity was examined numerically through non-linear static analyses. A description of the non-linear model and the different analyzed cases precedes, and the results of the analyses follows.

5.1 Non-linear Static Analyses

The material nonlinearity was taken into account using the Von Mises plasticity model, implemented in the DIANA FEA software [19]. An elastic-perfectly plastic constitutive relationship was adopted. The characteristic values considered are presented in Table 8, and included the material strength, as obtained by the

investigation campaign, including a confidence factor, and the density, the Modulus of Elasticity, the Poisson's ratio and ultimate strain, as generally assumed for steel material. The strain at yield was derived explicitly by the modulus of elasticity and the strength. Moreover, following the model updating procedure, the damage of the columns due to corrosion was modeled as an equivalent decrease of the modulus of elasticity. This simplification implied that the same decrease ratio was induced also for the strength of the columns. Therefore, the resulting stress-strain law followed a "strain-equivalence", as both strain at yield and ultimate remain the same.

Table 8. Adopted material properties of the final model.

Properties		Intact members	Damaged columns
Material density	ρ [kg/m^3]	7850	7850
Modulus of elasticity	E [GPa]	200	91.5
Poisson's ratio	ν	0.30	0.30
Yield strength	f_y [MPa]	226	103.5
Ultimate strain	ε_u	0.01	0.01

During each step of the non-linear analysis, an iterative process took place to guarantee equilibrium. This process employed the secant iteration method, while the equilibrium was ensured when the energy norm ratio was less than 0.001. In addition, the arc-length technique was used in order to improve convergence.

The integration points were set using the Gauss' scheme. For the case of the beam elements, two integration points were used along the axis of the elements, while 4x4 integration points were used over the cross-section. In the case of arbitrary sections, a distinct integration scheme was adopted for each individually defined area, by a 3x3 scheme. This mainly refers to the columns, and ended up with multiple integration points per section (e.g. a simple rectangular column with angles at the corners resulted in 108 integration points over the section). Concerning the shell elements, 2x2 integration points were used over the area, and three integration

points were used across the thickness of each leaf. The last number is considered sufficient due to especially limited thickness of each leaf of 1.08mm.

Several non-linear static (pushover) analyses were performed in order to conclude about the response and safety of the Basilica. More specifically, the response in the transversal direction, which was expected to be the most crucial, was examined under two different load patterns, namely a first-mode proportional pattern and a mass proportional pattern. Since the geometry and the numerical model of the Basilica are symmetric along the longitudinal axis, the analyses were performed only in one direction. It is noted that the actual structure is not perfectly symmetric, as highlighted by the presence of the second mode of the dynamic identification test, yet such local differentiations were neglected in this global model. The response in the longitudinal direction was examined under only a mass proportional load pattern, as a leading global mode in that direction was not identified neither by the experimental tests, nor by the numerical model. In this case, due to the lack of symmetry, the load was applied in both positive and negative directions.

Before each pushover analysis, the self-weight was applied. It should be noted that a self-weight verification was performed under increasing load (i.e. a push-down analysis), and the Basilica remained elastic, even for significantly higher gravitational loads. The results of this verification are not shown and the interested reader is referred to [20].

5.2 Analyses Results

The results of the analyses performed for the transversal direction are presented in Figure 16 (a) in terms of capacity curves. The horizontal axis corresponds to the displacement of the point of the roof highlighted in the plan of the structure, while the vertical axis corresponds to the ratio of the base shear reaction to the mass of the structure. The deformed shape of the structure for both the modal and the mass proportional load patterns at the last step of the analyses are presented in Figure 16 (b) and (c). Detailed results on the distribution of stresses and strain may be found in [20].

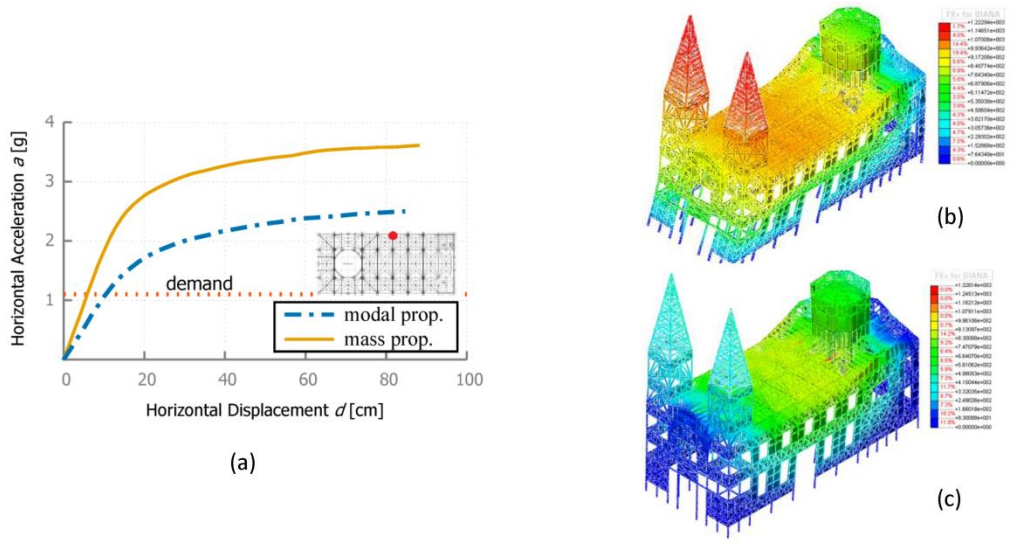

Figure 16. Results of the pushover analyses in the transversal direction: (a) capacity curves, and displacements of (b) mass and (c) modal proportional loading pattern, during the last step.

As expected, when the load is applied according to the modal pattern, the structure is more flexible and presents a lower force capacity, compared with the mass proportional pattern. In more details, in the case of the modal loading pattern, the capacity curve is almost elastic until a horizontal acceleration of around 1.5 g and reaches a maximum acceleration of 2.5 g. In the case of mass loading pattern, the structure behaves almost elastically until around 2.4 g and shows a maximum capacity of 3.6 g. It is of interest to underline that, independently of the load pattern, the equivalent yield displacement of the structure appears at the same displacement of the roof close to 18 cm, for both cases. The same applies for the ultimate displacement at 85 cm. Such an outcome indicates that in the non-linear range, displacements are a more consistent indicator of the extent of damage rather than forces, as has been discussed extensively by [29].

By comparing the deformed shapes and damage concentration of the structure for the two load patterns, a rather different response is observed. In the case of the mass proportional loading, the structure deforms fairly linearly up to the top part of the towers, while the part of the sanctuary deforms less, when compared horizontally. This is attributed to the fact that more load is applied at the façade of the Basilica, due to the additional mass of the towers, while central nave possesses

less stiffness from the outset. Furthermore, the elements that appear to be mainly stressed out and yield are the two transversal walls of the façade and the sanctuary, the columns in the central nave, and the roof trusses that connect the columns in the transversal direction. A crucial role is played by the stiffness and load path discontinuities that appear in the façade across the height, due to the presence of openings. In the case of the modal load pattern, the structure deforms mainly in the upper part of the central nave, in accordance with the 1st mode. In this case, there is slightly less yielding in the transversal braces and walls, while damage appears also in the vaulting system. This outcome indicates the action of the vaulting system as a flexible diaphragm, which provides redundancy to the structural system.

In parallel with the capacity curves, Figure 16 (a) also displays the spectral acceleration demand according to the National Structural Code of Philippines (NSCP) [30]. The site of the Basilica is expected to be subjected to a Peak Ground Acceleration (PGA) of 0.44 g, while since the structure has frequencies higher than 2.5 Hz, it falls in the constant acceleration plateau of the spectrum at 1.1 g, after considering the SDOF to MDOF transformation factor. By comparing the acceleration demand, it is clear that the Basilica is estimated to remain elastic, despite its significant deformation capacity. This outcome points out that the Basilica is in compliance with the code seismic safety requirements. At this point, it is important to underline that the verification is performed following a force-based approach, which is justified by the following notes: a) the stiffness of the Basilica has been specified after experimental tests, and not by arbitrary a priori considerations; b) nonlinearities of the structure are included explicitly in the analysis, and not with a simplified lumped approach; and c) the structure remains in the linear range and thus an obscure reduction factor is not required to verify the structure.

The results of the analyses performed in the longitudinal directions are presented in Figure 17 (a) in terms of capacity curves, and in Figure 17 (b) and (c) in terms of deformed shapes. Similarly with the results presented for the transversal direction, the vertical axis of the capacity curves has been normalized to the mass of the structure, and represents the horizontal acceleration.

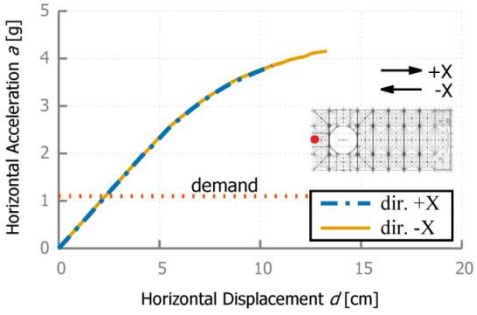

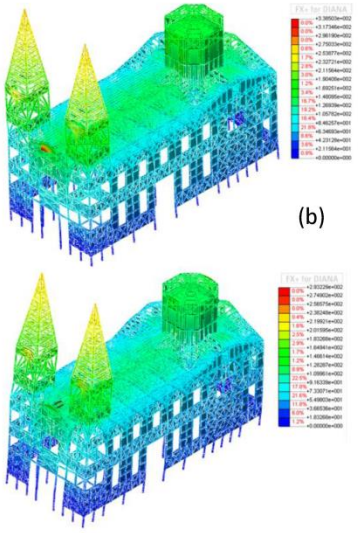

Figure 17. Results of the pushover analyses in the longitudinal direction: (a) capacity curves, and displacements in the (b) positive and (c) negative directions during the last step.

The capacity curves of the structure in the positive and negative longitudinal directions appear to be identical, up to the displacement of 11 cm. At that point, the analysis of the positive direction stops, while the analysis in the negative direction continues up to 13.3 cm. The lower capacity of the response in the positive direction is attributed to convergence difficulties due to local instabilities, rather than an earlier global collapse. Nevertheless, the structure appears to yield around 5.4 cm and 2.5 g, for both cases. Moreover, it can be clearly observed that the structure is much stiffer than the transversal direction, in line with the lack of a distinguishable global mode in this direction.

By observing the deformed shapes and damage extent, similar response is shown in both directions. More specifically, the deformations vary linearly up to the top of the structure, while a local amplification is observed in the tympanum of the façade. This last observation is attributed to the fact that this wall has a single leaf of 1.08 mm and therefore a small out-of-plane stiffness. The main resisting elements in the longitudinal direction are the longitudinal walls and braces, due to their high in-plane stiffness. However, once more the stiffness and load-path discontinuity of the windows at the base of the longitudinal facades leads to an equivalent soft-story response that drives the collapse.

Figure 17 (a) compares also the capacity curves with the acceleration demand of the NSCP. Similarly with the transversal direction, the structure is expected to remain in the elastic field, and thus complies with the seismic safety requirements. It should be noted that the longitudinal direction presents a higher safety factor than the transversal direction in terms of forces, but lower ductility. The former superiority is attributed to the higher plan inertia and the higher number of in-plane resisting elements (braces and walls); while the last disadvantage derives by the equivalent soft-story mechanism.

6. Conclusions

The present study investigated the seismic behavior of the San Sebastian Basilica in Philippines, a unique architectural heritage structure of the 19th century, made of steel. After an extensive investigation campaign, a step-by-step modeling approach was adopted in order to calibrate a detailed numerical model, based on the Finite Element Method, with the experimental tests. The seismic capacity was obtained by performing non-linear static analyses, and the safety of the Basilica was verified.

After presenting the historical context under which the Basilica was constructed, followed a description of its structural configuration. Since the architectural concept was an attempt to mimic the neo-gothic style, the moment resisting frame structural system was enriched with steel plates and diagonal braces, enhancing its performance. Then, the main outcomes of a versatile investigation campaign were presented, arriving to the dynamic identification tests recently performed. The main dynamic properties of the Basilica were estimated, including six modal frequencies, their modes shapes and the corresponding damping ratios.

Afterwards, starting with a simple numerical model that included the main structural components, a step-by-step approach was followed in order to derive a consisted model that compromises sophistication and simplicity. The later was then further manipulated according to a model updating method, so to replicate even in more detail the actual structure, as indicated by the experimental tests. The final numerical model, although not in perfect alignment with the experimental results,

was able to highlight its main characteristics and included also secondary elements and the existing damage due to corrosion of the steel.

Finally, the seismic assessment of the Basilica was performed through non-linear static analyses in the two main directions, considering the actual condition of the building. The transversal direction of the structure appeared to be the most flexible and weak in terms of forces, due to the lower density of diagonal braces and steel plates. Other components that appeared to have significant role on the seismic capacity of the Basilica are the diaphragmatic action that the vaulting system is offering, and the load-path and stiffness discontinuity along the height presented due to the openings. Nevertheless, the Basilica showed a satisfactory seismic capacity when compared to the seismic demand of the site, verifying its historical performance against earthquakes without any significant reported damage. It is noted that the second order effects of the steel elements (geometric nonlinearity), creep and pinching phenomena were not taken into account.

Closing, although the initial intention of the original building designer was to construct an “earthquake-proof” and “termite-proof” church was well stated and this was verified here by modern sophisticated numerical tools, yet the history has shown that the lack of a “corrosion-proof” system could hinder the first. The present study showed that in the current state there is no need for any global strengthening of the existing structure, but action should be taken against the active corrosion phenomena.

Acknowledgements

The support of the San Sebastian Basilica Conservation and Development Foundation, Inc. in providing access to the building and information on the Church is gratefully acknowledged. This work was partly funded by project STAND4HERITAGE that has received funding from the European Research Council (ERC) under the European Union’s Horizon 2020 research and innovation programme (Grant agreement No. 833123), as an Advanced Grant.

References

[1] P. Roca, P.B. Lourenço, A. Gaetani, Historic Construction and Conservation, Routledge, New York, 2019. https://doi.org/10.1201/9780429052767.

[2] ISCARSAH, Principles for the Analysis, Conservation and Structural Restoration of Architectural Heritage, Int. Counc. Monum. Sites. (2003) 3–6.

[3] P.B. Lourenço, Conservation of cultural heritage buildings: Methodology and application to case studies, Rev. ALCONPAT. 3 (2013) 101. https://doi.org/10.21041/ra.v3i2.46.

[4] M.P. Ciocci, S. Sharma, P.B. Lourenço, Engineering simulations of a super-complex cultural heritage building: Ica Cathedral in Peru, Meccanica. 53 (2018) 1931–1958. https://doi.org/10.1007/s11012-017-0720-3.

[5] L.C. Silva, N. Mendes, P.B. Lourenço, J. Ingham, Seismic Structural Assessment of the Christchurch Catholic Basilica, New Zealand, Structures. 15 (2018) 115–130. https://doi.org/10.1016/j.istruc.2018.06.004.

[6] S. Saloustros, L. Pelà, P. Roca, J. Portal, Numerical analysis of structural damage in the church of the Poblet Monastery, Eng. Fail. Anal. 48 (2015) 41–61. https://doi.org/10.1016/j.engfailanal.2014.10.015.

[7] A. Gebreyohaness, C. Clifton, J. Butterworth, Assessment of the seismic performance of old riveted steel frame-RC wall buildings, J. Constr. Steel Res. 75 (2012) 1–10. https://doi.org/10.1016/j.jcsr.2012.02.009.

[8] F. Marques, C. Moutinho, F. Magalhães, E. Caetano, Á. Cunha, Analysis of dynamic and fatigue effects in an old metallic riveted bridge, J. Constr. Steel Res. 99 (2014) 85–101. https://doi.org/10.1016/j.jcsr.2014.04.010.

[9] M. Pagani, J. Garcia-Pelaez, R. Gee, K. Johnson, V. Poggi, R. Styron, G. Weatherill, M. Simionato, D. Viganò, L. Danciu, D. Monelli, Global Earthquake Model (GEM) Seismic Hazard Map, Dec 05, 2018. (2018) v2018.1. https://doi.org/10.13117/GEM-GLOBAL-SEISMIC-HAZARD-MAP-2018.1.

[10] Save San Sebastian Basilica Conservation and Development Foundation Inc., San Sebastian Basilica: Final Conditions Assessment. Report SRP380-11-GR-146, Philippines, 2014.

[11] E.L.A. Romanillos, The Augustinian Recollects in the Philippines, Hagiography and History., Manila, Philippines, 2001.

[12] A. Cascardi, F. Micelli, M.A. Aiello, M.F. Funari, Structural analysis of a masonry church with variable cross-section dome, in: Brick Block Masonry-From Hist. to Sustain. Mason., 2020: pp. 220–226. https://doi.org/10.1201/9781003098508-28.

[13] N. Kassotakis, V. Sarhosis, B. Riveiro, B. Conde, A. Maria, D. Altri, J. Mills, G. Milani, S. De Miranda, G. Castellazzi, Automation in Construction Three-

dimensional discrete element modelling of rubble masonry structures from dense point clouds, Autom. Constr. 119 (2020). https://doi.org/10.1016/j.autcon.2020.103365.

[14] M.F. Funari, A.E. Hajjat, M.G. Masciotta, D. V Oliveira, P.B. Lourenço, A Parametric Scan-to-FEM Framework for the Digital Twin Generation of Historic Masonry Structures, Sustainability. 13 (2021). https://doi.org/10.3390/su131911088.

[15] SVS - Structural Vibration Solutions A/S, ARTeMIS Ambient Response Testing and Modal Identification Software, (2013).

[16] R. Brincker, C.E. Ventura, Introduction to Operational Modal Analysis, John Wiley & Sons., 2015. https://doi.org/10.1002/9781118535141.

[17] L.F. Ramos, Damage identification on masonry structures based on vibration signatures, PhD Thesis. (2007). https://doi.org/10.1038/nmat3777.

[18] MIDAS Information Technology Co Ltd, Midas FX+ for DIANA, Version 3.3.0, Korea, 2013.

[19] DIANA, User's Manual - Release 10.1, DIANA FEA BV., 2017. https://dianafea.com/manuals/d101/Diana.html.

[20] N. O'Hearne, Seismic safety assessment of the San Sebastian Basilica in Manila, Philippines, Università degli Studi di Pavia, 2017.

[21] G.L. Kulak, J.W. Fisher, J.H.A. Struik, Guide to design criteria for bolted and riveted joints, 2001.

[22] R.T. Leon, Seismic performance of bolted and riveted connections., in: Backgr. Reports Metall. Fract. Mech. Welding, Moment Connect. Fram. Syst. Behav., 1997: pp. 5.1-5.74.

[23] G.P. Forcier, R.T. Leon, B.E. Severson, C.W. Roeder, Seismic performance of riveted connections, J. Constr. Steel Res. 58 (2002) 779–799. https://doi.org/10.1016/S0143-974X(01)00097-9.

[24] R. Landolfo, L. Cascini, F. Portioli, Modeling of metal structure corrosion damage: A state of the art report, Sustainability. 2 (2010) 2163–2175. https://doi.org/10.3390/su2072163.

[25] B.M. Doublas, W.H. Reid, Dynamic tests and system identification of bridges, J. Struct. Div. 108 (1982) 2295–2312.

[26] C. Gentile, A. Saisi, Ambient vibration testing of historic masonry towers for structural identification and damage assessment, Constr. Build. Mater. 21 (2007) 1311–1321. https://doi.org/10.1016/j.conbuildmat.2006.01.007.

[27] F. Peña, P.B. Lourenço, N. Mendes, D. V. Oliveira, Numerical models for the seismic assessment of an old masonry tower, Eng. Struct. 32 (2010) 1466–1478. https://doi.org/10.1016/j.engstruct.2010.01.027.

[28] N. Mendes, Seismic Assessment of Ancient Masonry Buildings : Shaking Table Tests and Numerical Analysis, PhD Dissertation, Universidade do Minho, 2012.

[29] M.J.N. Priestley, G.M. Calvi, M.J. Kowalsky, Displacement Based Seismic Design of Structures, IUSS Press, Pavia, 2007.

[30] Association of Structural Engineers Philippines, National Structural Code of the Philippines 2010, (2010).